Am J Transl Res 2025;17(7):4952-4963
www.ajtr.org /ISSN:1943-8141/AJTR0163088

Original Article

Mesenchymal stem cells promote erlotinib resistance in non-small cell lung cancer through the HGF-AKT/ERK1/2-OPN pathway

Yue Yang[1,2*], Jianxin He[3*], Feng Long[3], Yongqi Liu[3], Li Lin[4], Hulai Wei[2]

[1]Key Laboratory of Environmental Ecology and Population Health in Northwest Minority Areas, State Ethnic Affairs Commission, Northwest Minzu University, Lanzhou 730000, Gansu, China; [2]Key Laboratory of Preclinical Study for New Drugs of Gansu Province, School of Basic Medical Sciences, Lanzhou University, Lanzhou 730000, Gansu, China; [3]Key Laboratory of Ministry of Education for Dunhuang Medicine and Transformation, Gansu University of Chinese Medicine, Lanzhou 730000, Gansu, China; [4]Department of Hematology and Oncology, Gansu Provincial Maternity and Child-Care Hospital, Lanzhou 730050, Gansu, China. [*]Equal contributors.

Received January 4, 2025; Accepted June 11, 2025; Epub July 15, 2025; Published July 30, 2025

Abstract: Objectives: To investigate the mechanisms by which mesenchymal stem cells (MSCs) contribute to erlotinib resistance in non-small cell lung cancer (NSCLC). Methods: HCC827 NSCLC cells were treated with MSC-conditioned medium (MSC-CM). Cell viability and apoptosis were evaluated using MTT assays and flow cytometry, respectively. Protein and mRNA expression levels were assessed by western blotting and quantitative real-time PCR. For *in vivo* validation, a xenograft model was established by co-injecting HCC827 cells and MSCs into NOD/SCID mice. Results: MSC-CM significantly increased cell viability and reduced apoptosis in HCC827 cells following erlotinib treatment, indicating enhanced drug resistance. Mechanistically, MSC-secreted hepatocyte growth factor (HGF) activated AKT and ERK1/2 phosphorylation, thereby bypassing EGFR inhibition by erlotinib. Neutralization of HGF restored erlotinib sensitivity in MSC-CM-treated HCC827 cells. Furthermore, osteopontin (OPN) was transcriptionally upregulated and acted as a resistance enhancer. Inhibition of OPN attenuated MSC-CM-mediated resistance. *In vivo*, tumors derived from co-injected MSCs and HCC827 cells exhibited significantly greater volume and weight after erlotinib treatment compared to control tumors. Conclusions: This study identifies a novel MSC-mediated resistance mechanism in which MSC-derived HGF activates compensatory AKT/ERK1/2 signaling, circumventing EGFR blockade by erlotinib. Concurrent upregulation of OPN in NSCLC cells forms a synergistic survival axis under erlotinib pressure. These findings suggest that targeting MSC-derived HGF and tumor-derived OPN may offer promising strategies to overcome erlotinib resistance in NSCLC.

Keywords: Mesenchymal stem cells, HCC827, erlotinib resistance, HGF-AKT/ERK1/2 signals, osteopontin

Introduction

Lung cancer remains the leading cause of cancer-related mortality worldwide, accounting for approximately 1.3 million deaths annually [1]. Histologically, it is classified into two major subtypes: non-small cell lung cancer (NSCLC) and small cell lung cancer (SCLC), with NSCLC comprising over 80% of cases and representing the primary contributor to lung cancer mortality [2, 3]. Although surgical resection and radiotherapy are curative options for early-stage NSCLC, most patients are diagnosed at advanced stages, where systemic chemotherapy becomes the standard treatment [4-6].

Activating somatic mutations in the epidermal growth factor receptor (EGFR) gene, accompanied by overexpression of mutant EGFR protein, are key oncogenic drivers in approximately 30% of NSCLC cases, making EGFR a critical therapeutic target [7-9]. First-generation EGFR tyrosine kinase inhibitors (TKIs), such as erlotinib and gefitinib, have demonstrated substantial efficacy in NSCLC patients harboring well-characterized EGFR-activating mutations, including the L858R point mutation and exon 19 deletions [10, 11]. Erlotinib functions by competitively binding to the ATP-binding site of EGFR, thereby inhibiting its tyrosine kinase activity and downstream AKT and ERK1/2 signaling

https://doi.org/10.62347/RKYL8675

cascades, ultimately inducing apoptosis in NSCLC cells [12].

However, acquired resistance to erlotinib typically emerges within 12 months of treatment, severely limiting its long-term clinical benefit [13]. Resistance mechanisms generally fall into three categories: (1) the EGFR T790M secondary mutation, which accounts for ~60% of resistant cases and reduces drug binding affinity; (2) epithelial-mesenchymal transition, which promotes cellular plasticity and EGFR-independent survival; and (3) stromal interactions within the tumor microenvironment that activate bypass pathways such as AKT and ERK1/2 [14-16].

Mesenchymal stem cells (MSCs), originally identified in bone marrow as multipotent stromal progenitors, possess differentiation potential toward osteoblasts, adipocytes, and epithelial cells under specific conditions [17]. Beyond their regenerative capacity, MSCs contribute to tumor progression by enhancing proliferation, modulating immune responses, promoting metastasis, and facilitating drug resistance. Notably, MSCs migrate to tumor sites and influence the microenvironment through secretion of cytokines and exosomes [18, 19]. Previous studies have shown that MSCs promote erlotinib resistance in NSCLC by secreting leptin and insulin-like growth factor-binding protein 2 (IGFBP2) [20], and they are also known to secrete hepatocyte growth factor (HGF), a key modulator of cancer progression [21, 22]. However, the specific role of MSC-derived HGF in mediating acquired resistance to erlotinib in EGFR-mutant NSCLC remains unclear.

In this study, we systematically investigated the paracrine effects of MSCs on erlotinib resistance using EGFR-mutant HCC827 NSCLC cells. We found that MSC-conditioned medium (MSC-CM) significantly increased cell viability and reduced apoptosis in erlotinib-treated HCC827 cells. Mechanistically, MSC-derived HGF activated MET receptor signaling, leading to phosphorylation of AKT (Ser473) and ERK1/2 (Thr202/Tyr204). This activation promoted transcription of the spp1 gene and enhanced secretion of osteopontin (OPN), establishing a compensatory HGF/OPN signaling loop that bypassed EGFR inhibition. Neutralization of HGF with a blocking antibody significantly restored erlotinib sensitivity. *In vivo*, xenograft models confirmed that MSC co-injection led to increased tumor growth under erlotinib treatment.

These findings reveal a novel MSC-mediated resistance mechanism in NSCLC involving paracrine activation of the HGF-AKT/ERK1/2-OPN axis. Targeting MSC-related secretomes, particularly HGF and OPN, may offer a promising strategy to overcome erlotinib resistance in EGFR-mutant NSCLC.

Materials and methods

EGFR-mutated NSCLC cell line

The EGFR-mutated NSCLC cell line HCC827, harboring an exon 19 deletion in the EGFR gene, was obtained from the Cell Bank of the Shanghai Institutes for Biological Sciences, Chinese Academy of Sciences (China). Cells were cultured in RPMI-1640 medium supplemented with 10% fetal bovine serum (FBS; BI, Israel).

Identification of MSCs

MSCs were purchased from Cyagen Biosciences (Guangzhou, China) and cultured in MSCM medium (ScienCell, San Diego, CA, USA) supplemented with 10% FBS at 37°C in a humidified incubator with 5% CO_2. Morphology was assessed under an AX80 optical microscope (Olympus, Tokyo, Japan).

MSCs were characterized by flow cytometry using surface markers CD73, CD166, CD29, CD44, CD34, CD45, and HLA-DR. Cells were stained with phycoerythrin (PE)-conjugated primary antibodies against these markers, along with an isotype control (Cyagen), followed by PE-labeled secondary antibodies (Cyagen). Data were analyzed using a BD Biosciences flow cytometer.

For osteogenic differentiation, MSCs were cultured in osteogenic induction medium (Cyagen) for two weeks, fixed with 4% paraformaldehyde, stained with Alizarin Red S, and visualized microscopically. For adipogenic differentiation, MSCs were cultured in adipogenic induction medium (Cyagen), followed by fixation and staining with Oil Red O.

Preparation of MSC-CM

MSCs (1×10^6) were seeded in a 10-cm dish with MSCM and cultured for 24 h. After washing

Table 1. Sequences of the primers

Gene name	Primer
spp1	Forward primer (5'-3'): ATGATTCTCACCAGTCTGA
	Reverse primer (5'-3'): TGTGGGGACAACTGGAGTG
HGF	Forward primer (5'-3'): TCAGTATCCTCACGAGCAT
	Reverse primer (5'-3'): CTCGGATGTTTGGATCAGT
FGF2	Forward primer (5'-3'): AGCTACAACTTCAAGCAGAA
	Reverse primer (5'-3'): CACATTTAGAAGCCAGTAAT
GAPDH	Forward primer (5'-3'): GGGCTCTCCAGAACATCAT
	Reverse primer (5'-3'): GGGACACGGAAGGCCATGC

twice with PBS, cells were incubated with 15 mL RPMI-1640 medium without FBS for an additional 24 h. The medium was collected, filtered through a 0.22 μm sterile filter, and stored at -80°C for further use.

MTT assay

HCC827 cells (5×10^3) were seeded in 24-well plates and incubated with or without MSC-CM supplemented with 10% FBS for 24 h, followed by treatment with erlotinib (0.01-0.11 μM; Toronto Research Chemicals, Canada) for 72 h. MTT (0.5 mg/mL) was added and incubated for 4 h. Formazan crystals were solubilized with DMSO, and absorbance was measured at 490 nm using a Victor X microplate reader (PerkinElmer).

Cell apoptosis analysis

HCC827 cells (1×10^5) were pretreated with or without MSC-CM for 24 h and then exposed to 0.05 μM erlotinib for 48 h. After collection and PBS wash, cells were stained with 4 μL Annexin V-FITC and 2 μL propidium iodide in 200 μL binding buffer (BestBio, Beijing, China) and analyzed by flow cytometry (BD Biosciences, NJ, USA).

Western blotting

HCC827 cells (1×10^5) were cultured with or without MSC-CM and treated with 0.01, 0.05, or 0.09 μM erlotinib for 48 h. Cells were lysed using RIPA buffer (Solarbio, China), and proteins were extracted by centrifugation (12,000 rpm, 10 min, 4°C). Equal amounts of protein (5 μg) were separated by 12% SDS-PAGE and transferred to PVDF membranes (Millipore, USA). Membranes were probed with the following primary antibodies: p-EGFR (#48576), EGFR (#4267), p-AKT (#4060), AKT (#4691), p-ERK1/2 (#8544), ERK1/2 (#4695) (Cell Signaling Technology, USA); HGF (ab178395), OPN (ab8448) (Abcam, China); GAPDH (10494-1-AP, Proteintech, Beijing, China). HRP-conjugated secondary antibodies (ZB-2301, ZSGB-Bio, Beijing, China) were used, and detection was performed using an enhanced chemiluminescence reagent (Millipore).

Quantitative real-time PCR

Total RNA from MSCs and HCC827 cells was extracted using an RNAprep Pure Cell Kit (TIANGEN, Beijing, China), and cDNA synthesis was conducted using the EasyScript Reverse Transcriptase Kit (TAKARA, Kyoto, Japan). qPCR was performed on a CFX96 Real-Time PCR System (Bio-Rad, USA) using SYBR® Premix Ex Taq™ II (TAKARA). Cycling conditions: 95°C for 3 min, followed by 40 cycles of 95°C for 15 s, 60°C for 30 s, and 72°C for 30 s. Gene expression levels of HGF, fibroblast growth factor 2 (FGF2), and OPN were normalized to GAPDH using the $2^{-\Delta\Delta CT}$ method. Primer sequences are listed in **Table 1**.

ELISA assay

MSCs and HCC827 cells were cultured in serum-free RPMI-1640 medium for 24 h. The supernatants were collected, and HGF concentrations were measured using an ELISA kit (Jianglai Biotechnology, China), according to the manufacturer's instructions.

Gene chip assay

HCC827 cells (1×10^5) were incubated with RPMI-1640 or MSC-CM (supplemented with 10% FBS) for 48 h. Total RNA was extracted, and mRNA expression profiling was performed using the Affymetrix PrimeView Human Gene Expression Array (CapitalBio, Beijing, China). Briefly, 100 ng of RNA per sample was reverse-transcribed, and biotin-labeled cRNA was synthesized and hybridized. The arrays were processed using the Affymetrix Fluidics Station 450 and scanned with a GeneChip Scanner 3000 7G. Data were normalized with the Robust Multiarray Average (RMA) algorithm. Differentially expressed genes were identified

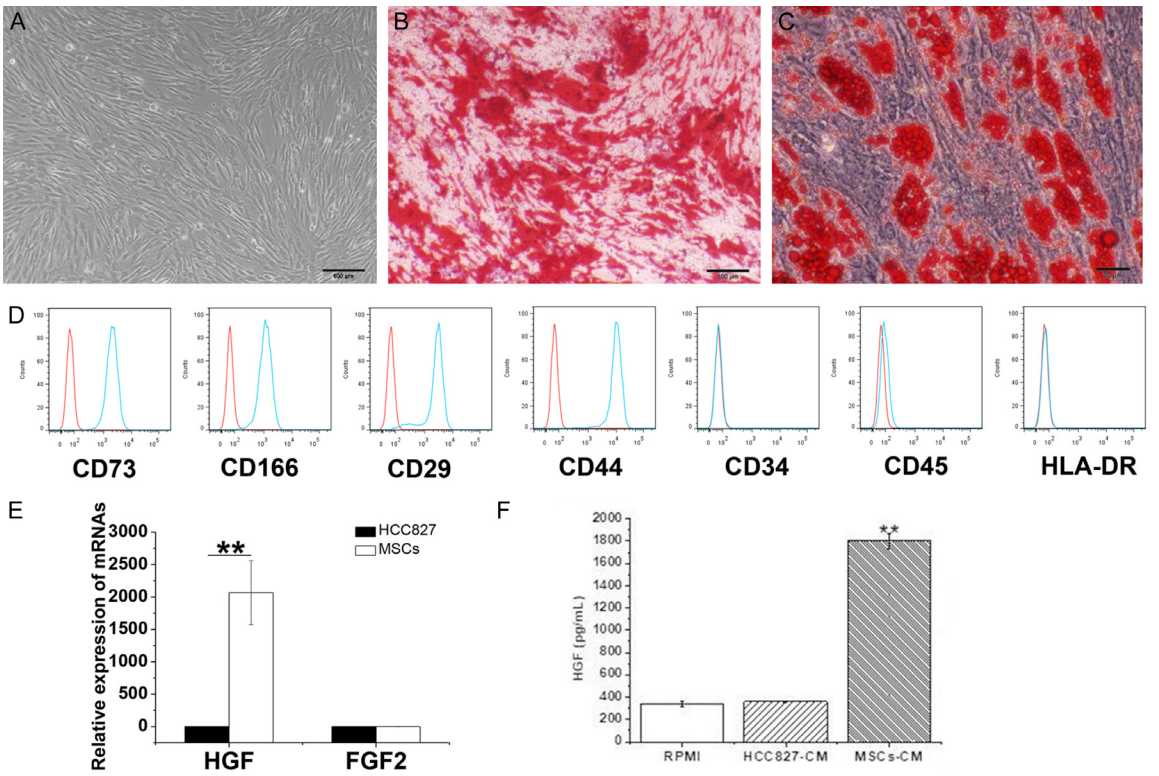

Figure 1. Characterization and identification of MSCs. A. Morphologic features of MSCs observed by light microscopy (×100). B. Osteogenic differentiation of MSCs assessed by Alizarin Red S staining (×100). C. Adipogenic differentiation of MSCs assessed by Oil Red O staining (×400). D. Surface marker expression of MSCs analyzed by flow cytometry. E. Quantitative real-time PCR analysis of HGF and FGF2 mRNA expression in MSCs and HCC827 cells. **P<0.01. F. ELISA measurement of HGF protein levels secreted by MSCs and HCC827 cells. **P<0.01. MSCs: mesenchymal stem cells.

based on fold change and false discovery rate thresholds.

Xenograft experiments

Eight-week-old female NOD/SCID mice (n=16, ~22 g each) were purchased from Vital River (Beijing, China). All procedures were conducted in specific pathogen-free conditions following GB/T 35892-2018 guidelines and approved by the Animal Ethics Committee of Lanzhou University (approval no. LZUSBMS-EAAC-2018-008).

Mice were randomized into four groups (n=4 each): HCC827 alone, HCC827 + erlotinib, MSCs alone, and HCC827 + MSCs + erlotinib. Cells (1×10^6 HCC827, MSCs, or both) were subcutaneously injected into the flanks. When tumors reached ~80 mm^3, erlotinib (25 mg/kg/day) was administered orally every three days for 28 days. Mice were anesthetized with 5% isoflurane (RWD, Shenzhen, China) and euthanized via cervical dislocation. Tumor volume was calculated as (length × $width^2$)/2 and measured weekly. Final tumor weights were recorded at sacrifice.

Statistical analysis

Data were presented as mean ± standard deviation (SD) based on three independent experiments. Statistical analyses were conducted using one-way ANOVA, with significance set at P<0.05. Variances were assessed with Post-hoc Test (Least Significant Difference). SPSS13.0 was used for data analysis.

Results

Characterization and identification of MSCs

The morphology and phenotypic markers of MSCs were analyzed. MSCs exhibited a uniform spindle-shaped morphology and adhered to the culture surface (**Figure 1A**). Alizarin Red S stain-

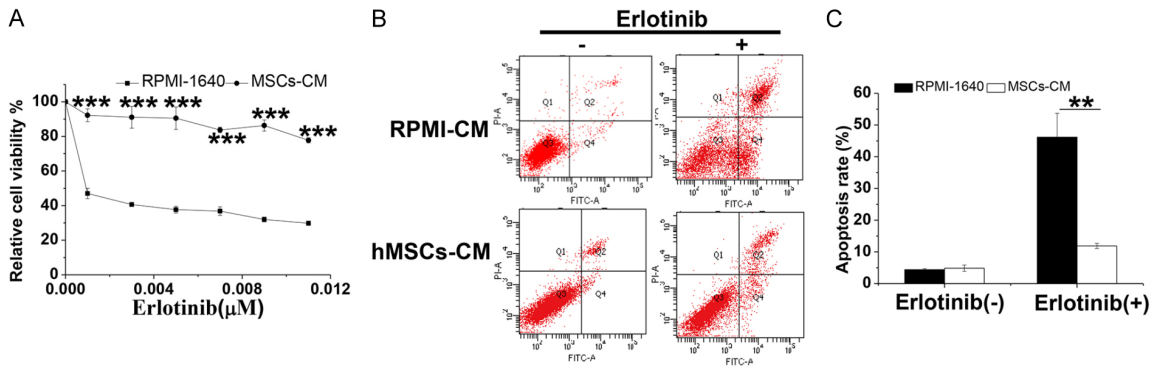

Figure 2. MSC-CM enhances erlotinib resistance in HCC827 cells. A. HCC827 cells cultured in either RPMI-1640 or MSC-CM were treated with increasing concentrations of erlotinib for 72 h. Cell viability was assessed using the MTT assay. ***P<0.001 vs. RPMI-1640 group. B. HCC827 cells cultured in RPMI-1640 or MSC-CM were treated with 0.05 μM erlotinib for 48 h, followed by apoptosis analysis via flow cytometry. C. Quantification of apoptotic rates in each group. **P<0.01 vs. RPMI-1640 group. MSC-CM: Mesenchymal stem cell-conditioned medium.

ing (**Figure 1B**) and Oil Red O staining (**Figure 1C**) confirmed their capacity for osteogenic and adipogenic differentiation under specific induction. Flow cytometry showed that MSCs were positive for CD73, CD166, CD29, and CD44, but negative for CD34, CD45, and HLA-DR (**Figure 1D**), consistent with established MSC phenotypes [23].

MSCs are known to constitutively secrete HGF and FGF2 [24, 25]. Real-time quantitative PCR revealed significantly higher mRNA levels of HGF in MSCs compared to HCC827 cells, while FGF2 mRNA levels were similar in both cell types (**Figure 1E**). ELISA confirmed a higher level of HGF secretion in MSCs than in HCC827 cells (**Figure 1F**).

MSC-CM enhances erlotinib resistance in HCC827 cells

To assess the effect of MSCs on erlotinib sensitivity, HCC827 cells were cultured in MSC-CM and treated with varying concentrations of erlotinib. Cell viability assays showed that MSC-CM significantly enhanced the survival of HCC827 cells under erlotinib treatment compared to RPMI-1640 controls (P<0.001) (**Figure 2A**). Flow cytometry revealed that erlotinib-induced apoptosis was markedly reduced in MSC-CM-treated cells compared to controls (P<0.01) (**Figure 2B** and **2C**), suggesting that MSC-CM confers partial resistance to erlotinib.

MSCs-secreted HGF induces AKT and ERK1/2 activation, mediating erlotinib resistance

EGFR activation typically triggers downstream c-MET phosphorylation and activates the PI3K-AKT and MAPK-ERK1/2 signaling pathways, contributing to chemoresistance [26, 27]. To investigate these signaling events, we examined the phosphorylation status of EGFR (Tyr1068), AKT (Ser473), and ERK1/2 (Thr202/Tyr204) in HCC827 cells cultured in RPMI-1640 versus MSC-CM following erlotinib treatment.

Western blot analysis revealed increased phosphorylation of AKT and ERK1/2 in MSC-CM-treated cells compared to RPMI-1640 controls (both P<0.05, **Figure 3A-D**). In both conditions, EGFR phosphorylation was significantly reduced upon 0.05 μM erlotinib treatment (P<0.01), confirming its inhibitory effect on EGFR. In RPMI-1640 conditions, AKT phosphorylation decreased with increasing erlotinib concentration, while in MSC-CM, AKT remained activated despite treatment, indicating EGFR-independent AKT activation. Similarly, ERK1/2 phosphorylation was consistently higher in MSC-CM-treated cells under all erlotinib concentrations.

HGF directly engages its transmembrane c-Met receptor on cancer cells to activate the AKT-ERK1/2 signaling cascade, thus inducing cancer cells to develop resistance to chemo-

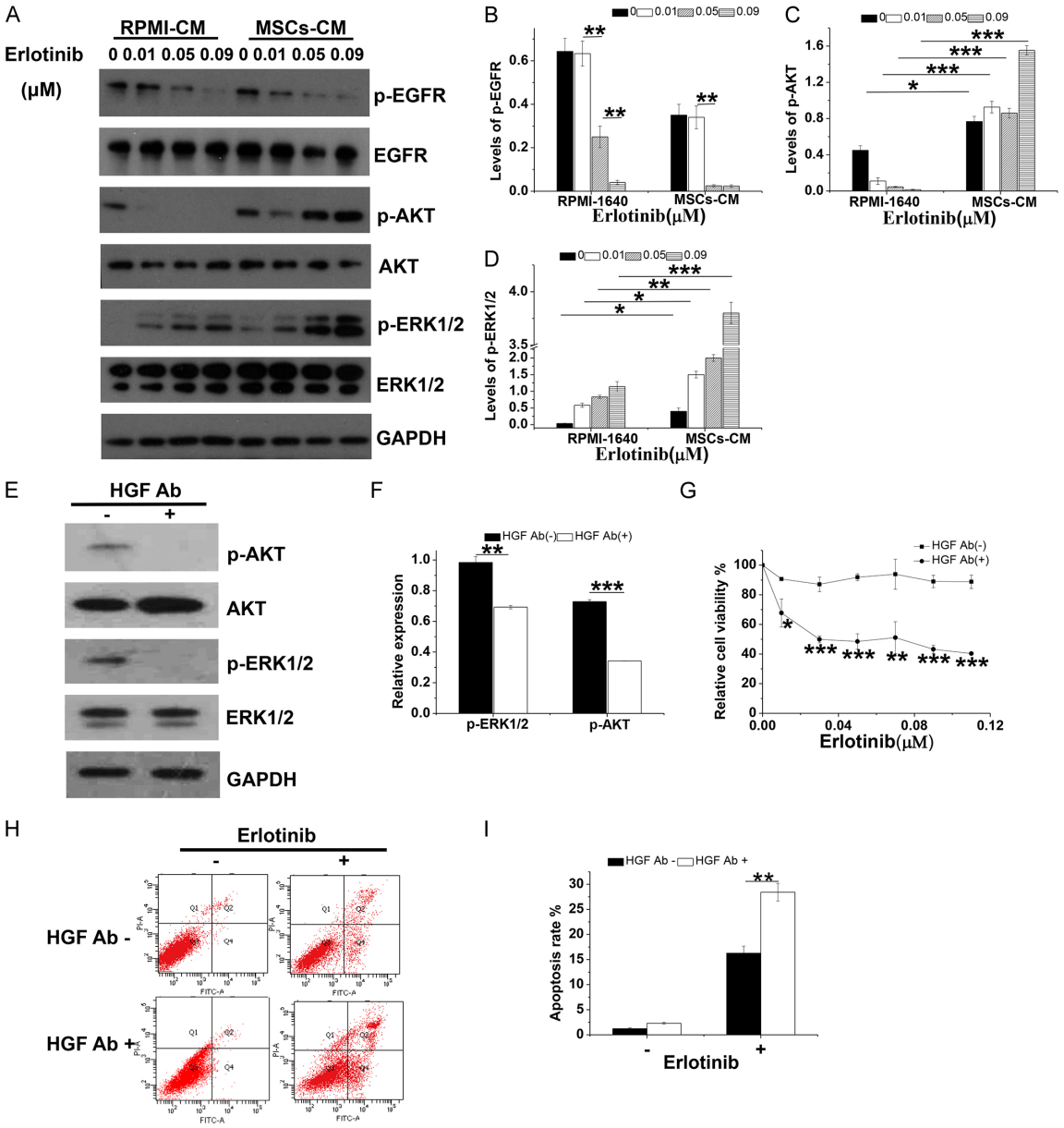

Figure 3. MSC-secreted HGF t induces AKT and ERK1/2 activation, mediating erlotinib resistance. A. HCC827 cells cultured in RPMI-1640 or MSC-CM were treated with varying concentrations of erlotinib for 36 h. The levels of phosphorylated EGFR (p-EGFR), STAT3 (p-STAT3), AKT (p-AKT), and ERK1/2 (p-ERK1/2) were detected by western blotting. B-D. Quantification of p-EGFR, p-AKT, and p-ERK1/2 expression. *P<0.05, **P<0.01, ***P<0.001. E. MSC-CM-cultured HCC827 cells were treated with 20 ng/mL HGF neutralizing antibody for 24 h, followed by western blotting to assess p-AKT and p-ERK1/2 levels. F. Quantification of p-AKT and p-ERK1/2 levels in each group. **P<0.01, ***P<0.001. G. MSC-CM-cultured HCC827 cells were treated with increasing concentrations of erlotinib with or without 20 ng/mL HGF antibody for 72 h. Cell viability was measured using the MTT assay. *P<0.05, **P<0.01, ***P<0.001 vs. HGF Ab (-) group. H. MSC-CM-cultured HCC827 cells were treated with 0.05 μM erlotinib with or without 20 ng/mL HGF antibody for 48 h. Apoptosis was analyzed by flow cytometry. I. Quantification of apoptotic rates. **P<0.01. MSC-CM: Mesenchymal stem cell-conditioned medium, HGF: hepatocyte growth factor.

therapy [28, 29]. To validate HGF's role in this pathway, HCC827 cells were treated with MSC-CM in the presence of an HGF polyclonal antibody (HGF-pAb). Phosphorylation levels of AKT (P<0.001) and ERK1/2 (P<0.01) were markedly reduced after HGF neutralization (**Figure 3E** and **3F**), confirming HGF as the upstream activator.

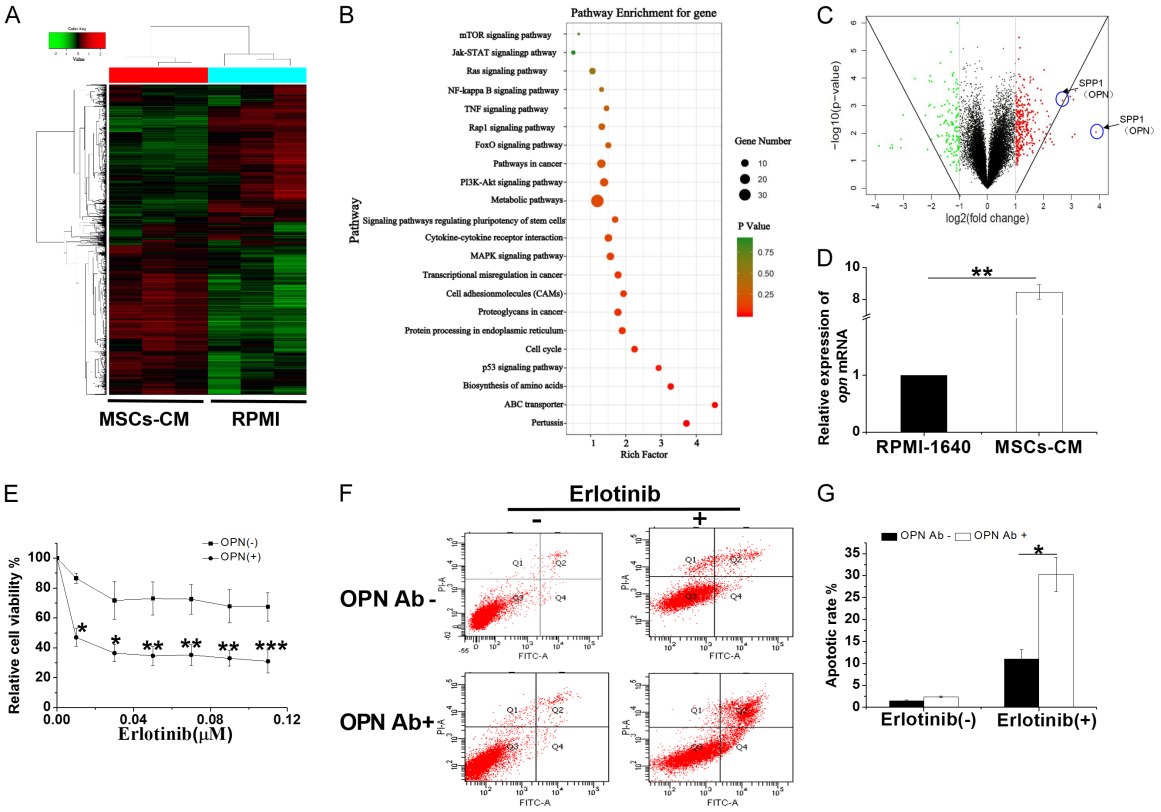

Figure 4. MSC-CM upregulates the drug resistance-associated gene SPP1 in HCC827 cells. A. Heatmap of differentially expressed genes between MSC-CM and RPMI-1640-cultured HCC827 cells. B. KEGG pathway enrichment analysis of differentially expressed genes presented as a bubble plot. C. Volcano plot of differentially expressed genes. D. Relative OPN mRNA expression levels in the two groups. **P<0.01. E. MSC-CM-cultured HCC827 cells were treated with varying concentrations of erlotinib with or without 20 ng/mL OPN neutralizing antibody for 72 h. Cell viability was measured by MTT assay. *P<0.05, **P<0.01, ***P<0.001 vs. OPN Ab (-). F. MSC-CM-cultured HCC827 cells were treated with 0.05 μM erlotinib with or without 20 ng/mL OPN antibody for 48 h, and apoptosis was assessed by flow cytometry. G. Quantification of apoptotic rates in each group. *P<0.05. MSC-CM: Mesenchymal stem cell-conditioned medium, OPN: osteopontin.

Co-treatment with erlotinib and HGF-pAb significantly reduced the viability of MSC-CM-treated HCC827 cells (P<0.05) (**Figure 3G**) and synergistically enhanced apoptosis, as demonstrated by flow cytometry (P<0.01) (**Figure 3H** and **3I**).

MSC-CM induces expression of SPP1 in HCC827 cells

To further investigate the molecular mechanisms underlying MSC-induced resistance, we performed transcriptomic profiling with a microarray in HCC827 cells cultured in RPMI-1640 versus MSC-CM. A total of 452 differentially expressed genes were identified, including 312 upregulated and 140 downregulated transcripts. The heatmap illustrates clustering of differentially expressed genes (**Figure 4A**), and the top 20 are listed in **Table 2**. KEGG pathway analysis revealed enrichment in the PI3K-AKT and MAPK signaling pathways (**Figure 4B**).

Notably, among the top seven upregulated genes, two paralogs of SPP1 (encoding OPN) were identified as associated with therapy resistance (**Figure 4C**). qPCR confirmed significantly elevated OPN mRNA levels (P<0.01) in MSC-CM-treated HCC827 cells compared to controls (**Figure 4D**).

To determine whether OPN contributes to erlotinib resistance, HCC827 cells were treated with erlotinib in combination with an anti-OPN antibody. Co-treatment significantly reduced cell viability in MSC-CM-cultured cells (P<0.05, **Figure 4E**). Flow cytometry analysis showed that anti-OPN antibody enhanced erlotinib-

Table 2. List of top 20 upregulated and top 20 downregulated genes in HCC827 cells cultured with MSC-conditioned medium versus RPMI-1640, ranked by fold change

No.	Gene Symbol	Fold Change	q-value (%)	Gene Symbol	Fold Change	q-value (%)
1	SPP1	14.6524	0	NABP1	0.4979	3.3337449
2	CEACAM6	8.4068	0	NAMPT	0.4973	0.0738251
3	TSPAN8	5.1575	0	SPIRE1	0.4968	0.0146381
4	FGFBP1	4.9372	0	ETV5	0.4963	0
5	HPGD	4.7348	0	CASP4	0.496	0
6	ERP27	4.7102	0	AARS	0.4954	0
7	CFI	4.5289	0	TCEA1	0.4951	0
8	ARL6IP1	4.3651	0	GTPBP2	0.495	0.0583879
9	METTL7A	4.3611	0	UBE2H	0.4942	0.0583879
10	TMEM27	4.0607	0	ETS1	0.4935	0
11	FGB	3.9558	0.03921903	PGBD5	0.4915	0
12	STS	3.9556	0	PTPDC1	0.4914	0.5062998
13	RNF128	3.8785	0	TXNIP	0.4897	0.5653746
14	SLC30A1	3.7497	0	C1S	0.4881	0
15	CYP26A1	3.5758	0	FOSL1	0.4877	0
16	ST8SIA4	3.457	0	PHLDB2	0.4866	0.8944021
17	DPP4	3.4515	0	C3	0.4862	0
18	AQP3	3.2729	0	SLC7A11	0.4853	0
19	ALCAM	3.2547	0	MAP1LC3B	0.4848	0.0287065
20	HMMR	3.2302	0	CREB5	0.4844	0

induced apoptosis by 2.3-fold (P<0.05) (**Figure 4F** and **4G**), supporting a functional role for OPN in resistance.

MSC-induced erlotinib resistance in HCC827 cells in vivo

To validate the in vitro findings, a xenograft model was used to evaluate MSC-mediated erlotinib resistance *in vivo*. Tumor volume and weight were significantly reduced in mice treated with erlotinib compared to untreated HCC827 controls (both P<0.05, **Figure 5A-C**). However, in mice co-injected with MSCs and HCC827 cells, erlotinib treatment resulted in significantly larger tumor volume (P<0.05) and weight (P<0.01) compared to the erlotinib-only group. Notably, no tumors formed in the MSC-only group.

Discussion

Mesenchymal stem cells (MSCs) can migrate to various tumor types and act as facilitators of tumor progression by promoting metastasis, enhancing angiogenesis, and inducing immunosuppression [30, 31]. In addition, MSCs have been shown to contribute to acquired chemoresistance in multiple malignancies through stromal-tumor interactions mediated by cytokines and exosomes [32-34]. However, the role of MSCs in conferring resistance to erlotinib in NSCLC remains underexplored. In this study, we conducted both *in vitro* and *in vivo* experiments to investigate the effects of MSCs on erlotinib resistance in the EGFR-mutant NSCLC cell line HCC827.

MSCs secrete a range of cytokines and exosomes that influence tumor drug responses [18]. We hypothesized that MSCs could promote chemoresistance in HCC827 cells by cytokine-mediated mechanisms. To test this, HCC827 cells were cultured in MSC-CM, and their response to erlotinib was compared with cells cultured in standard RPMI-1640 medium. HCC827 cells in MSC-CM exhibited increased viability and reduced apoptosis upon erlotinib treatment, indicating that MSC-derived soluble factors confer cytoprotection through paracrine signaling. Among the cytokines implicated in tumor-associated resistance, HGF is known to be secreted by MSCs and other cell types [35, 36]. Our data demonstrate that MSCs promote

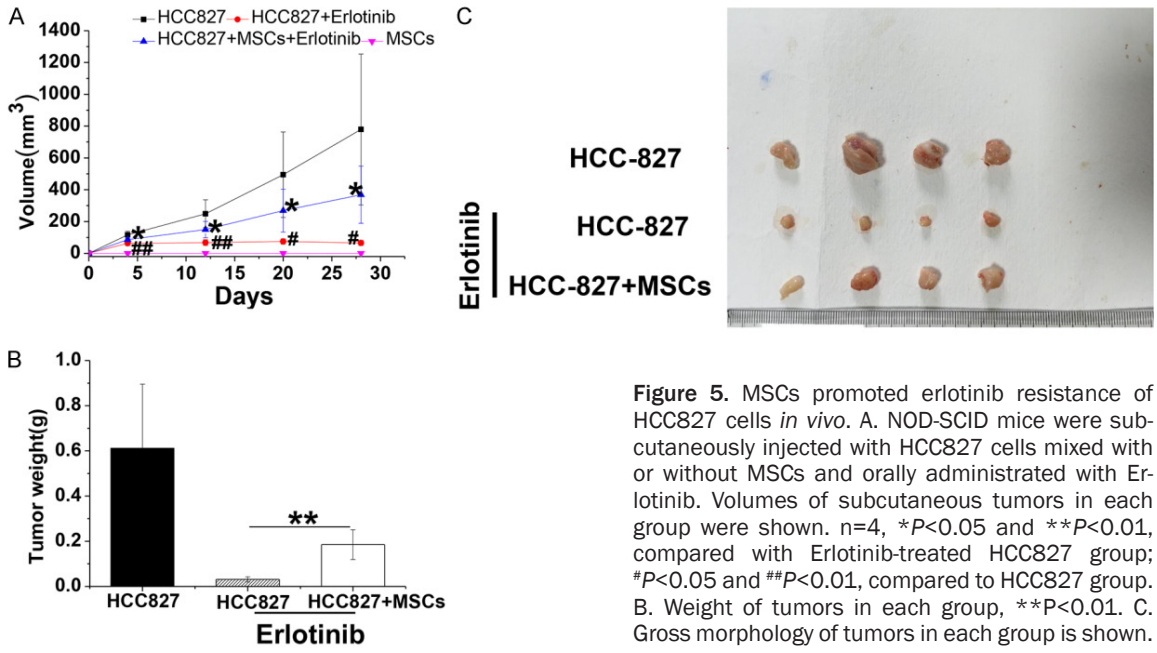

Figure 5. MSCs promoted erlotinib resistance of HCC827 cells *in vivo*. A. NOD-SCID mice were subcutaneously injected with HCC827 cells mixed with or without MSCs and orally administrated with Erlotinib. Volumes of subcutaneous tumors in each group were shown. n=4, **P*<0.05 and ***P*<0.01, compared with Erlotinib-treated HCC827 group; #*P*<0.05 and ##*P*<0.01, compared to HCC827 group. B. Weight of tumors in each group, **P<0.01. C. Gross morphology of tumors in each group is shown.

erlotinib resistance in NSCLC cells via HGF secretion, consistent with prior findings that HGF mediates resistance to EGFR-TKIs in NSCLC cell lines [37].

To explore the underlying mechanism, we focused on EGFR downstream signaling. In HCC827 cells, mutant EGFR is constitutively active and drives the PI3K-AKT and MAPK-ERK1/2 signaling pathways [27, 38]. We found that MSC-CM significantly increased the phosphorylation of AKT and ERK1/2, even in the absence of erlotinib. Upon erlotinib treatment, AKT and ERK1/2 phosphorylation remained elevated in MSC-CM-treated cells compared to controls, suggesting that MSC-derived factors bypass EGFR blockade and directly activate survival pathways.

Given that both HGF and FGF have been implicated in drug resistance in NSCLC [39, 40], and that HGF in particular activates the PI3K-AKT axis [41], we compared HGF mRNA expression in MSCs and HCC827 cells. MSCs exhibited significantly higher HGF expression. To directly assess the role of HGF, MSC-CM was pretreated with a neutralizing anti-HGF antibody. This intervention suppressed AKT and ERK1/2 phosphorylation and decreased cell viability while increasing apoptosis, demonstrating that HGF is a critical mediator of MSC-induced resistance. These findings indicate that MSC-derived HGF activates AKT/ERK1/2 signaling in HCC827 cells, overriding erlotinib's inhibitory effects on the EGFR pathway.

To further delineate the molecular basis of this resistance, we performed transcriptomic analysis of HCC827 cells cultured in RPMI-1640 versus MSC-CM. A total of 452 differentially expressed genes were identified, with 312 upregulated and 140 downregulated. Among the top upregulated genes was SPP1, encoding OPN, a secreted matrix glycoprotein involved in tumor growth, metastasis, and chemoresistance [42, 43]. Previous studies have shown that HGF can induce SPP1 expression through the PI3K-AKT pathway [44]. Consistent with this, MSC-CM significantly increased OPN mRNA expression in HCC827 cells, suggesting that HGF/AKT signaling mediates SPP1 upregulation. Neutralization of OPN with a specific antibody restored sensitivity to erlotinib, as evidenced by reduced viability and increased apoptosis in MSC-CM-treated HCC827 cells. These results suggest that OPN is a downstream effector of the HGF-AKT/ERK1/2 axis, contributing to erlotinib resistance.

We further validated these findings *in vivo* using a xenograft model. MSCs alone did not form tumors, confirming their non-tumorigenic phenotype in NOD/SCID mice. Instead of systemic injection, MSCs were co-injected subcutaneously with HCC827 cells to establish a local tumor microenvironment and avoid systemic

degradation of HGF. Erlotinib treatment significantly inhibited tumor growth in the HCC827-only group, reducing both tumor volume and weight. However, co-injection of MSCs with HCC827 cells led to substantial attenuation of erlotinib efficacy, confirming that MSCs mediate erlotinib resistance *in vivo*. Notably, no tumors developed in the MSC-only group, confirming the stromal, rather than oncogenic, role of MSCs in this context.

In conclusion, our findings reveal a novel mechanism of MSC-induced erlotinib resistance in NSCLC. MSCs establish a paracrine HGF/OPN axis that activates AKT/ERK1/2 phosphorylation and upregulates SPP1 expression, thereby bypassing EGFR-dependent signaling and promoting drug resistance in HCC827 cells. These results highlight the MSC secretome as a key contributor to acquired resistance and suggest that targeting the HGF-OPN axis may offer a new therapeutic strategy for overcoming EGFR-TKI resistance in NSCLC.

Acknowledgements

This work was supported by the National Natural Science Foundation of China [number 81503377], Industry Support Plan Project of Gansu Provincial Department of Education [number 2022CYZC-54] and Open Foundation of Key Laboratory of Dunhuang Medicine and Transformation [number DHYX18-10], Scientific Research Fund for Talent Introduction of Northwest Minzu University [number xbmuyjrc202235], the Fundamental Research Funds for the Central Universities [number 31920250061] and the University Fund for Young Doctors of Gansu Province [number 2022QB027].

Disclosure of conflict of interest

None.

Address correspondence to: Hulai Wei, Key Laboratory of Preclinical Study for New Drugs of Gansu Province, School of Basic Medical Sciences, Lanzhou University, No. 199 Donggang West Road, Chengguan District, Lanzhou 730000, Gansu, China. Tel: +86-13893158796; E-mail: weihulai_2024@126.com

References

[1] Sung H, Ferlay J, Siegel RL, Laversanne M, Soerjomataram I, Jemal A and Bray F. Global cancer statistics 2020: GLOBOCAN estimates of incidence and mortality worldwide for 36 cancers in 185 countries. CA Cancer J Clin 2021; 71: 209-249.

[2] Kleczko EK, Kwak JW, Schenk EL and Nemenoff RA. Targeting the Complement pathway as a therapeutic strategy in lung cancer. Front Immunol 2019; 10: 954.

[3] Alexander M, Kim SY and Cheng H. Update 2020: management of non-small cell lung cancer. Lung 2020; 198: 897-907.

[4] Gustin P, Botticella A, Tselikas L, Mercier O, Le Pechoux C and Levy A. Therapeutic options for oligoprogressive non-small cell lung cancer. Rev Mal Respir 2019; 36 :519-526.

[5] Park K, Wan-Teck Lim D, Okamoto I and Yang JC. First-line afatinib for the treatment of EGFR mutation-positive non-small-cell lung cancer in the 'real-world' clinical setting. Ther Adv Med Oncol 2019; 11: 1758835919836374.

[6] Jonna S and Subramaniam DS. Molecular diagnostics and targeted therapies in non-small cell lung cancer (NSCLC): an update. Discov Med 2019; 27: 167-170.

[7] Holleman MS, van Tinteren H, Groen HJ, Al MJ and Uyl-de Groot CA. First-line tyrosine kinase inhibitors in EGFR mutation-positive non-small-cell lung cancer: a network meta-analysis. Onco Targets Ther 2019; 12: 1413-1421.

[8] Hulo P, Coupez D, Denis MG and Bennouna J. EGFR mutation-positive NSCLC: factors to consider when deciding first-line therapy. Expert Rev Anticancer ther 2020; 20: 365-372.

[9] Dong RF, Zhu ML, Liu MM, Xu YT, Yuan LL, Bian J, Xia YZ and Kong LY. EGFR mutation mediates resistance to EGFR tyrosine kinase inhibitors in NSCLC: from molecular mechanisms to clinical research. Pharmacol Res 2021; 167: 105583.

[10] Nguyen CTT, Petrelli F, Scuri S, Nguyen BT and Grappasonni I. A systematic review of pharmacoeconomic evaluations of erlotinib in the first-line treatment of advanced non-small cell lung cancer. Eur J Health Econ 2019; 20: 763-777.

[11] Wang C, Zhao K, Hu S, Dong W, Gong Y, Li M and Xie C. Clinical outcomes of gefitinib and erlotinib in patients with NSCLC harboring uncommon EGFR mutations: a pooled analysis of 438 patients. Lung Cancer 2022; 172: 86-93.

[12] Abourehab MAS, Alqahtani AM, Youssif BGM and Gouda AM. Globally approved EGFR inhibitors: insights into their syntheses, target kinases, biological activities, receptor interactions, and metabolism. Molecules 2021; 26: 6677.

[13] Johnson M, Garassino MC, Mok T and Mitsudomi T. Treatment strategies and outcomes for patients with EGFR-mutant non-small cell lung cancer resistant to EGFR tyrosine kinase inhibitors: focus on novel therapies. Lung cancer 2022; 170: 41-51.

[14] Wilson TR, Fridlyand J, Yan Y, Penuel E, Burton L, Chan E, Peng J, Lin E, Wang Y, Sosman J, Ribas A, Li J, Moffat J, Sutherlin DP, Koeppen H, Merchant M, Neve R and Settleman J. Widespread potential for growth-factor-driven resistance to anticancer kinase inhibitors. Nature 2012; 487: 505-9.
[15] He J, Huang Z, Han L, Gong Y and Xie C. Mechanisms and management of 3rd-generation EGFR-TKI resistance in advanced non-small cell lung cancer (review). Int J Oncol 2021; 59: 90.
[16] Adachi Y, Ito K, Hayashi Y, Kimura R, Tan TZ, Yamaguchi R and Ebi H. Epithelial-to-mesenchymal transition is a cause of both intrinsic and acquired resistance to KRAS G12C inhibitor in KRAS G12C-mutant non-small cell lung cancer. Clin Cancer Res 2020; 26: 5962-5973.
[17] Liu J, Gao J, Liang Z, Gao C, Niu Q, Wu F and Zhang L. Mesenchymal stem cells and their microenvironment. Stem Cell Res Ther 2022; 13: 429.
[18] Lin Z, Wu Y, Xu Y, Li G, Li Z and Liu T. Mesenchymal stem cell-derived exosomes in cancer therapy resistance: recent advances and therapeutic potential. Mol Cancer 2022; 21: 179.
[19] Tu Z and Karnoub AE. Mesenchymal stem/stromal cells in breast cancer development and management. Semin Cancer Biol 2022; 86: 81-92.
[20] Wang F, Zhang L, Sai B, Wang L, Zhang X, Zheng L, Tang J, Li G and Xiang J. BMSC-derived leptin and IGFBP2 promote erlotinib resistance in lung adenocarcinoma cells through IGF-1R activation in hypoxic environment. Cancer Biol Ther 2020; 21: 61-71.
[21] Lu Z, Chang W, Meng S, Xu X, Xie J, Guo F, Yang Y, Qiu H and Liu L. Mesenchymal stem cells induce dendritic cell immune tolerance via paracrine hepatocyte growth factor to alleviate acute lung injury. Stem Cell Res Ther 2019; 10: 372.
[22] Eterno V, Zambelli A, Pavesi L, Villani L, Zanini V, Petrolo G, Manera S, Tuscano A and Amato A. Adipose-derived Mesenchymal Stem Cells (ASCs) may favour breast cancer recurrence via HGF/c-Met signaling. Oncotarget 2014; 5: 613-33.
[23] Naji A, Eitoku M, Favier B, Deschaseaux F, Rouas-Freiss N and Suganuma N. Biological functions of mesenchymal stem cells and clinical implications. Cell Mol Life Sci 2019; 76: 3323-3348.
[24] Han KH, Kim MH, Jeong GJ, Kim AK, Chang JW and Kim DI. FGF-17 from hypoxic human Wharton's Jelly-derived mesenchymal stem cells is responsible for maintenance of cell proliferation at late passages. Int J Stem Cells 2019; 12: 279-290.
[25] Usunier B, Brossard C, L'Homme B, Linard C, Benderitter M, Milliat F and Chapel A. HGF and TSG-6 released by mesenchymal stem cells attenuate colon radiation-induced fibrosis. Int J Mol Sci 2021; 22: 1790.
[26] Dent P, Booth L, Poklepovic A, Von Hoff D, Martinez J, Zhou Y and Hancock JF. Osimertinib-resistant NSCLC cells activate ERBB2 and YAP/TAZ and are killed by neratinib. Biochem Pharmacol 2021; 190: 114642.
[27] Yuan S, Chen W, Yang J, Zheng Y, Ye W, Xie H, Dong L and Xie J. Tumor-associated macrophage-derived exosomes promote EGFR-TKI resistance in non-small cell lung cancer by regulating the AKT, ERK1/2 and STAT3 signaling pathways. Oncol Lett 2022; 24: 356.
[28] Chen H, Lin C, Peng T, Hu C, Lu C, Li L, Wang Y, Han R, Feng M, Sun F and He Y. Metformin reduces HGF-induced resistance to alectinib via the inhibition of Gab1. Cell Death Dis 2020; 11: 111.
[29] Raghav KP, Gonzalez-Angulo AM and Blumenschein GR Jr. Role of HGF/MET axis in resistance of lung cancer to contemporary management. Transl Lung Cancer Res 2012; 1: 179-93.
[30] Huang C, Chen B, Wang X, Xu J, Sun L, Wang D, Zhao Y, Zhou C, Gao Q, Wang Q, Chen Z, Wang M, Zhang X, Xu W, Shen B and Wei Zhu W. Gastric cancer mesenchymal stem cells via the CXCR2/HK2/PD-L1 pathway mediate immunosuppression. Gastric Cancer 2023; 26: 691-707.
[31] Zhang LN, Zhang DD, Yang L, Gu YX, Zuo QP, Wang HY, Xu J and Liu DX. Roles of cell fusion between mesenchymal stromal/stem cells and malignant cells in tumor growth and metastasis. FEBS J 2021; 288: 1447-1456.
[32] Wu H, Mu X, Liu L, Wu H, Hu X, Chen L, Liu J, Mu Y, Yuan F, Liu W and Zhao Y. Bone marrow mesenchymal stem cells-derived exosomal microRNA-193a reduces cisplatin resistance of non-small cell lung cancer cells via targeting LRRC1. Cell Death Dis 2020; 11: 801.
[33] Zhang G, Miao F, Xu J and Wang R. Mesenchymal stem cells from bone marrow regulate invasion and drug resistance of multiple myeloma cells by secreting chemokine CXCL13. Bosn J Basic Med Sci 2020; 20: 209-217.
[34] Mehraj U, Dar AH, Wani NA and Mir MA. Tumor microenvironment promotes breast cancer chemoresistance. Cancer chemother Pharmacol 2021; 87: 147-158.
[35] Pour FK, Gale Dari MA, Ramazii M, Keivan M and Farzaneh M. Mesenchymal stem cells-con-

ditioned medium; an effective cell-free therapeutic option for *in vitro* maturation of oocytes. Curr Stem Cell Res Ther 2024; 19: 636-643.
[36] Nicu C, O'Sullivan JDB, Ramos R, Timperi L, Lai T, Farjo N, Farjo B, Pople J, Bhogal R, Hardman JA, Plikus MV, Ansell DM and Paus R. Dermal adipose tissue secretes hgf to promote human hair growth and pigmentation. J Invest Dermatol 2021; 141: 1633-1645, e13.
[37] Holland WS, Chinn DC, Lara PN Jr, Gandara DR and Mack PC. Effects of AKT inhibition on HGF-mediated erlotinib resistance in non-small cell lung cancer cell lines. J Cancer Res Clin Oncol 2015; 141: 615-26.
[38] Li H, Tong F, Meng R, Peng L, Wang J, Zhang R and Dong X. E2F1-mediated repression of WNT5A expression promotes brain metastasis dependent on the ERK1/2 pathway in EGFR-mutant non-small cell lung cancer. Cell Mol Life Sci 2021; 78: 2877-2891.
[39] Yi Y, Zeng S, Wang Z, Wu M, Ma Y, Ye X, Zhang B and Liu H. Cancer-associated fibroblasts promote epithelial-mesenchymal transition and EGFR-TKI resistance of non-small cell lung cancers via HGF/IGF-1/ANXA2 signaling. Biochim Biophys Acta Mol Basis Dis 2018; 1864: 793-803.
[40] Ware KE, Marshall ME, Heasley LR, Marek L, Hinz TK, Hercule P, Helfrich BA, Doebele RC and Heasley LE. Rapidly acquired resistance to EGFR tyrosine kinase inhibitors in NSCLC cell lines through de-repression of FGFR2 and FGFR3 expression. PLoS One 2010; 5: e14117.
[41] Fu R, Jiang S, Li J, Chen H and Zhang X. Activation of the HGF/c-MET axis promotes lenvatinib resistance in hepatocellular carcinoma cells with high c-MET expression. Med Oncol 2020; 37: 24.
[42] Liu K, Hu H, Jiang H, Zhang H, Gong S, Wei D and Yu Z. RUNX1 promotes MAPK signaling to increase tumor progression and metastasis via OPN in head and neck cancer. Carcinogenesis 2021; 42: 414-422.
[43] Fu Y, Zhang Y, Lei Z, Liu T, Cai T, Wang A, Du W, Zeng Y, Zhu J, Liu Z and Huang J. Abnormally activated OPN/integrin αVβ3/FAK signalling is responsible for EGFR-TKI resistance in EGFR mutant non-small-cell lung cancer. J Hematol Oncol 2020; 13: 169.
[44] Chen HT, Tsou HK, Chang CH and Tang CH. Hepatocyte growth factor increases osteopontin expression in human osteoblasts through PI3K, Akt, c-Src, and AP-1 signaling pathway. PLoS One 2012; 7: e38378.